



Supervised classification of down-hole physical properties measurements using neural network to predict the lithology



Omid Mahmoodi *, Richard S. Smith, Douglas K. Tinkham

Department of Earth Sciences, Laurentian University, Sudbury, ON P3E 2C6, Canada

ARTICLE INFO

Article history:

Received 11 March 2015

Received in revised form 4 November 2015

Accepted 10 November 2015

Available online 11 November 2015

Keywords:

Victoria

Down-hole

Physical properties

Neural network

Lithology

Physical unit

ABSTRACT

The reliability of rock-type prediction using down-hole density, gamma ray response, and magnetic susceptibility measurements was evaluated at the Victoria property, Sudbury, ON. A supervised neural network, trained using lithological information from drill hole FNX1168, yields a predictive accuracy of 83% for the training data. Applying the trained network on drill hole FNX1182 resulted in 64% of the rock types being correctly classified when compared with the classification produced by geologists during logging of the core. The homogenous rock types, like quartz diorite, had a high accuracy of classification; while the heterogeneous rock types such as diabase were poorly classified. Overlap between physical properties of rock types caused by heterogeneity or inherent similarity in physical properties of rock types, which were verified by observing the cores, accounts for most of the misclassification. To reduce the misclassification, the network was trained from physical log units in FNX1168 derived from clustering of physical properties measurements. Four physical log units mainly represented four groups of rocks: i) quartz diorite; ii) metabasalt and metagabbro; iii) metasediment and quartzite; and iv) sulfide and diabase. The predictive accuracy in the training process rose to 95%. The trained network then was applied to predicting the physical log units in FNX1182. Given the relationships between physical log units and rock types from FNX1168, the results of physical-log-unit classification in FNX1182 were interpreted from a geological point of view. Although in ideal cases we would like to be able to extract the same classification that a geologist provides, the extraction of physical log units is a more realistic goal. The interpretation of the lithological units from the physical log units can be compared with the geologist's classification and discrepancies or anomalies analyzed in greater detail.

© 2015 Elsevier B.V. All rights reserved.

1. Introduction

Typically when a hole is drilled, a geologist will look at the core extracted and classify the lithology or rock type as a function of depth down the hole. Rock type prediction based on log data from down-hole geophysical measurements can be considered as a potential alternative to a geologist's log when the cores are not fully recovered such as ocean drilling or drilling methods which do not provide cores such as percussion drilling in mineral exploration (Benaouda et al., 1999 and Qi and Carr, 2006). Physical properties logging provides a continuous set of data down the hole, which can be effectively used to improve the understanding of the geological characteristics of the hole (Killeen, 1997; McDowell et al., 1988; Granek, 2011). The accuracy of rock-type characterization based on physical properties is proportional to the existent contrast of these data between rock types (Perron et al., 2011 and Mwenifumbo and Mwenifumbo, 2012). But, similarity of physical properties of rocks and the heterogeneity of the rock increases the overlap

between physical properties of different rocks (Rabaute et al., 2003; Garcia et al., 2011). Overlap of physical properties between two rocks brings confusion to the prediction of rock types. We feel that it is more realistic to classify them as physical units. The term "physical log units" can be described as homogenous intervals of one or more rock types with consistent physical properties. The link between physical units and rock types can help geophysical studies to gain a better understanding of the geological setting (Benaouda et al., 1999 and Perron et al., 2011).

Conventional statistical techniques such as using histograms, box and whisker plots, cross plots, or the analysis of average and variance, were employed by Reed et al. (1997); Killeen (1997); McDowell et al. (1988, 2004), and Vella and Emerson (2009) to extract the pattern of variation in physical properties measurements and relate them to a geological setting. Recently, the multi-variable pattern recognition techniques have become popular, since the conventional methods were limited in terms of the number of variables, and their ability to establish a quantitative relationship between physical properties and a geological setting (Rabaute et al., 2003; Qi and Carr, 2006; Williams and Dipple, 2007; Garcia et al., 2011 and Granek, 2011). Supervised classification techniques can be used when the goal is to predict rock types based

* Corresponding author.

E-mail addresses: omahmoodi@laurentian.ca (O. Mahmoodi), rsmith@laurentian.ca (R.S. Smith), dtinkham@laurentian.ca (D.K. Tinkham).

on the physical properties measurements. As the term ‘supervised’ implies, a drill hole or parts of a hole with both physical properties measurement and rock type information are used to train the classifier, and then the trained classifier can be applied to a new hole or those parts lacking the core to predict the rock types (Benaouda et al., 1999 and Qi and Carr, 2006).

Varying composition of rock types, structures, alteration and mineralization cause non-linear variation in physical properties, which justifies using a non-linear classifier to analyze these data. The neural network is a robust non-linear classifier successfully applied to down-hole logging data (Ojha and Maiti, 2013). Baldwin et al. (1990); Wong et al. (1995); Farmer and Adams (1998); Qi and Carr (2006) and Maiti et al. (2007) used the neural network to predict lithofacies based on down-hole physical properties measurements. In these works a quantitative relationship between numerical well log data and core description is simulated by the neural network, then the network is applied to the uncored wells or parts of the well lacking the core to predict lithofacies. The application of a neural network was introduced to the Ocean Drilling Program by Benaouda et al. (1999) and Ojha and Maiti (2013). They used the neural network to classify down-hole physical properties measurement to predict lithology where there is partial or zero core recovery along the hole. All of the above mentioned works have been applied in the sedimentary environment, and the prediction was considered fairly successful. Application of this method to the igneous and metamorphic environments like the Victoria property might be complicated as they are more complex than sedimentary environments due to the structural metamorphic and intrusive history.

In this research, the main objective is to compare the reliability of representing the physical properties measurements in the form of rock types and physical log units. As a first step, a neural network trained from physical properties and geological logging information collected in hole FNX1168 was used to predict the rock type in hole FNX1182. If the network was trained on the data from more than one hole, better results might be obtained, but our purpose is to test the efficacy of neural networks early in the exploration process when less data are available. The predicted rock types in FNX1182 are compared with actual rock types logged by geologists to evaluate the accuracy of the classification in the context of an igneous and metamorphic environment. With the physical properties measurements available to us, we demonstrate below that this is only moderately successful. Then rather than using the geologists’ classification of rock units for training, we used physical log units in FNX1168 determined by fuzzy k-means clustering (Mahmoodi and Smith, 2015). The trained neural network was then used to predict physical units in FNX1182, with greater success. Considering the relationship between physical units and rock types is known for FNX1168, the predicted physical units of FNX1182 can be interpreted from a geological point of view. Finally, we discuss whether to represent down-hole physical properties measurements; in the form of rock type or physical log units.

2. Methods

The neural network is structurally comprised of an input layer, at least one hidden layer, and an output layer. Each layer has different numbers of neurons. Neurons of two adjacent layers are connected one-by-one by synaptic weights. The schematic structure of a simple three-layer neural network is shown in Fig. 1. The input data are represented as a data vector to the input layer. The number of neurons in the input layer equals the number of variables measured at each depth (in our case three, gamma-ray response, density and magnetic susceptibility). The number of output neurons is determined by the number of elements of the target vector; which is the number of classes in the classification problems (in our case seven rock types). The hidden neurons are computing elements of the network, which use transfer functions to generate the output. The input of a hidden neuron is a summation of bias and neurons in the previous layer multiplied by

corresponding synaptic weights. Biases allow the activation function to shift to the right or left to give a desired output (Bishop, 1995; Duda, 2001; Theodoridis and Koutroumbas, 2003 and Beale et al., 2001). In multilayer networks, the sigmoid function shown in Fig. 1 is often used as the transfer function (Beale et al., 2001). There is no rigorous theoretical method available to choose the number of hidden layers and hidden neurons, and they are often determined subjectively based on trial and error. The most compact structure with acceptable performance is preferred for computational efficiency. Most classification problems can be solved by the network when one hidden layer is used. With increase in the complexity of the relationship between input and desired output on the training data, the number of the hidden neurons should increase (Lawrence et al., 1996; Wong et al., 1995 and Beale et al., 2001).

The initial weights are randomly assigned to start the training process. The main task in network training is to adjust the weights to minimize the error of the network. The error function for each iteration is a form of the difference between the actual network output and the desired or target output. Here, mean square error (*mse*) is described as the error function:

$$J = mse = \frac{1}{N} \sum_{i=1}^N (e_i)^2 = \frac{1}{N} \sum_{i=1}^N (t_i - a_i)^2 \quad (1)$$

where t and a represent desired and network output respectively for each neuron of the output layer for N training data. In our case N is the number of depths that physical properties are measured at. A gradient descent is an optimization method which is used to adjust the weights in the direction through which the most rapid decrease in error function is achieved. The adjusting term ($\Delta\omega_j^r$), which is added to the j^{th} weight of the r^{th} layer weight after iteration, is obtained by the derivative (gradient) of the error function with respect to the weight. To enhance optimization efficiency, this value is multiplied by a learning rate (lr). The learning rate which is greater than zero and smaller than or equal to 1 controls the speed of the convergence process and how much the weights and biases can be modified at each iteration. The new estimate of the weight $\omega_{j(new)}^r$ is described as:

$$\omega_{j(new)}^r = \omega_{j(old)}^r - lr \cdot \Delta\omega_j^r, \quad \Delta\omega_j^r = \frac{\partial J}{\partial \omega_j^r}, \quad (2)$$

where $\omega_{j(old)}^r$ is the current weight, $\Delta\omega_j^r$ is the adjusting term, and lr is learning rate. The network with adjusted weights generates a new output set, and the process iterates (each iteration referred to as one epoch) until the termination criteria is fulfilled. Different criteria have been suggested to terminate the iterations, such as a threshold for the minimum performance function (cost function), the minimum decrease in the cost function in successive iterations, and the number of validation checks, which is the number of successive iterations that the cost function fails to decrease (Bishop, 1995; Benaouda et al., 1999; Theodoridis and Koutroumbas, 2003 and Beale et al., 2001).

The training data set must be sufficiently large to provide enough data to train and test the network. The data set is typically randomly divided into three parts for training, validation, and testing, constituting 70, 15, and 15% of the available data, respectively. Testing data are used to assess generalization of the trained network which determines capability of the network to be efficiently applied to new data. If the network keeps iterating and adjusting the parameters to minimize the error, the network starts to over-fit the training data. Over-fitting occurs when the network, irrespective of generalization, tries to minimize the error of training data. In this case, the impact of random noise is incorporated into the network weights; however, the error in testing and validation rises. Validation data is used to assure that the division of data is appropriate. If the errors of testing and validation data are significantly different, it indicates poor data division (Bishop, 1995; Benaouda et al.,

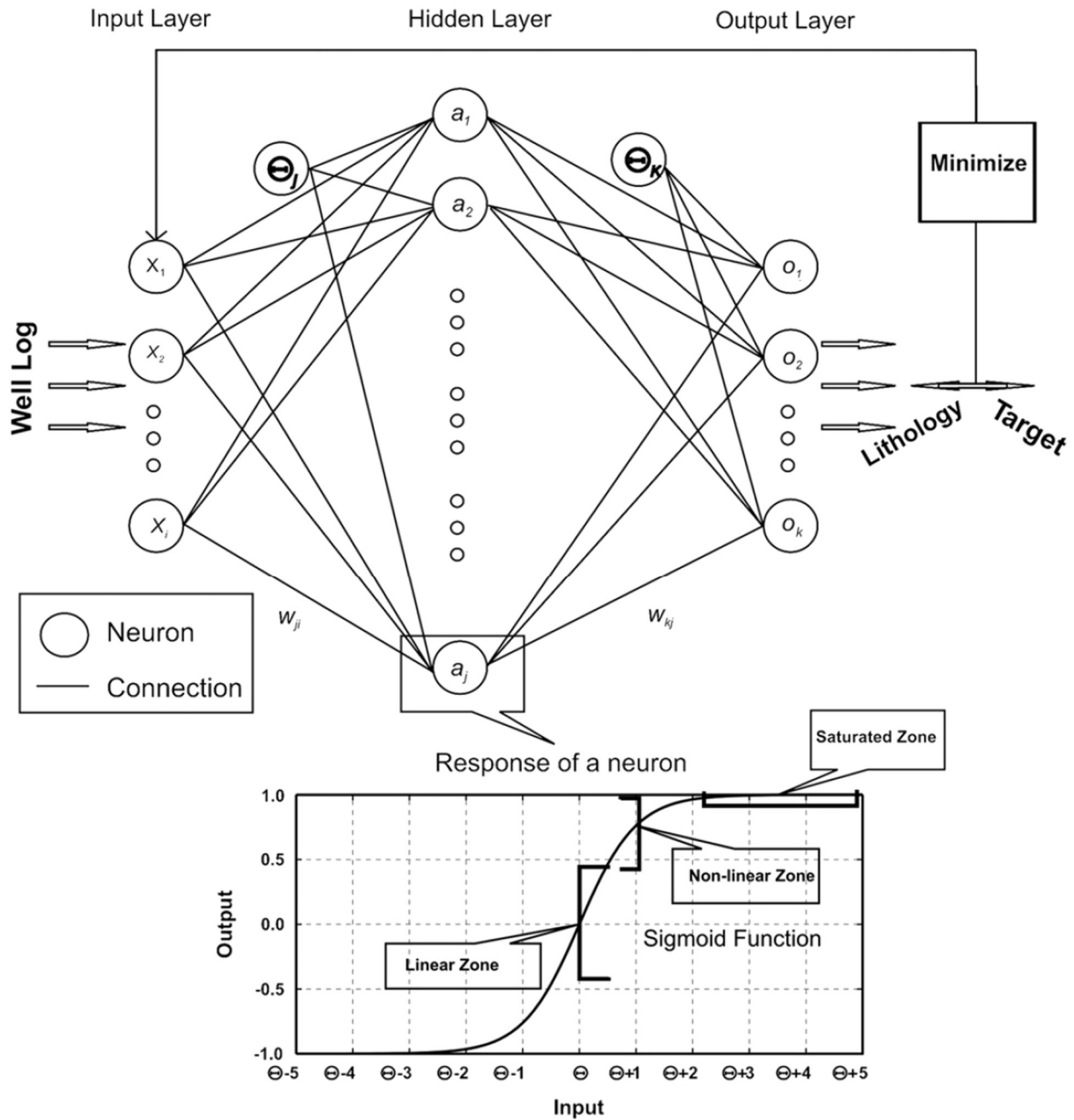


Fig. 1. The structure of a three-layer neural network. The well log data are presented to the input layer as vectors where x_i represents the i^{th} variable in an input data vector. Each input neuron is connected to neurons of the hidden layer by synaptic weights. Summation of input neuron multiplied by weights with bias added are fed to hidden neurons, a_1 to a_j represented by sigmoid function. The hidden neurons produce output which is input for the output layer. The sigmoid function, used as a transform function, is shown in the bottom of the figure. The bias neurons of the k^{th} layer are shown as θ_k . The output layer has k neurons which is equal to the number of classes in the target vector. In the training process, the network parameters are adjusted in an iterative manner to minimize the difference between the output of network and the target vector (Reprinted from Deep-Sea Res. II, Ojha and Maiti, Sediment classification using neural networks: An example from the site-U1344A of IODP Expedition 323 in the Bering Sea, Copyright (2013), with permission from Elsevier).

1999; Theodoridis and Koutroumbas, 2003; Qi and Carr, 2006 and Beale et al., 2001).

The MATLAB neural network toolbox was used to train the network, and then predict rock types and physical log units. The training process was carried out with 1000 iterations, 10 validation checks, a learning rate of 0.01, and a minimum gradient of 1×10^{-5} , as well as a performance goal of 0.03 for rock type prediction. These parameters are suggested by Lawrence et al. (1996) to avoid overfitting the network. A performance goal of 0.001 was used for physical unit prediction to take a longer time to train the network.

3. Data set used

The neural networks are not capable of extrapolating accurately beyond the range of data; hence, training and new data should have the same range (Beale et al., 2001). Therefore, training data and new data should be collected from one drillhole or a different hole drilled in the area with a similar geological setting. This will guarantee the consistency of the physical properties of the rocks and their relation to the rock type in the two datasets. In the current work, density, gamma-ray response, and magnetic susceptibility measured within FNx1168 and

FNX1182 drilled at the Victoria property were used. Fig. 2 shows the location of FNX1168 on the geological map of the Victoria property. FNX1182 is located to the north beyond the area covered by this map but is interpreted to intersect at depth the same geological units as appearing in FNX1168.

The boreholes were theoretically NQ sized (diameter of 75.7 mm), but the caliper log was measured to implement on-site calibration to correct for borehole size. The fluid filling the holes was water. A winch and steel cable system was used to lower a multi-parameter digital logging probe down the holes and measure the data. The data includes 4405 and 8484 measurement at an interval of 20 cm along the FNX1168 and FNX1182 holes, respectively.

We undertook the neural network training and classification process on the logging data from FNX1168 twice, firstly with the target vector as the rock type logged by geologists and secondly with the target as the physical log units identified by the fuzzy k-means clustering (Mahmoodi and Smith, 2015). The rock types logged by geologists in FNX1182 are only used to compare with the prediction from the trained networks. The physical properties measurements, rock type logged by geologists, and physical log units of FNX1168 are shown in Fig. 3.

The three-element input vectors representing three logging measurements at each depth were created. As is required in neural networks, each physical property should be normalized between 0 and 1. Because the magnetic susceptibility and gamma-ray response cover a large range of values, we found we could get better results when we took the logarithm of the measured value prior to normalizing the data. Each input vector of FNX1168 is then associated with a target vector identifying the rock type or physical unit belonging to each

measurement point. The number of elements in the target vector equals the number of classes present in training data; i.e. seven elements for rock types and four elements for physical units. The k^{th} element of the target vector is 1 when an input vector belongs to the k^{th} class, and the rest are 0 (Qi and Carr, 2006 and Beale et al., 2001).

4. Results

Precise training is a very important step in the classification of data using the neural network. Great care should be taken when selecting input variables from the available data set; the number of input data should be sufficient to allow the network to be trained properly. In neural network classification, the structure of the network is of significant importance. The network with the most compact and simplest structure is generally selected to classify new data as this provides minimal error and greatest generalization. This process is not straightforward; it requires considerable experimentation and evaluation of the error of performance and generalization of the network with different structures to obtain the optimal choice (Qi and Carr, 2006). Generally the required number of hidden layers and hidden neurons increase as the complexity between input and output data increases.

4.1. Predicting geological units

After some experimentation, the structure of the network for rock type prediction was selected to be 3–15–7. These values represent the number of neurons in the input layer, hidden layer, and output layer, respectively. In the training process the best performance occurred at the

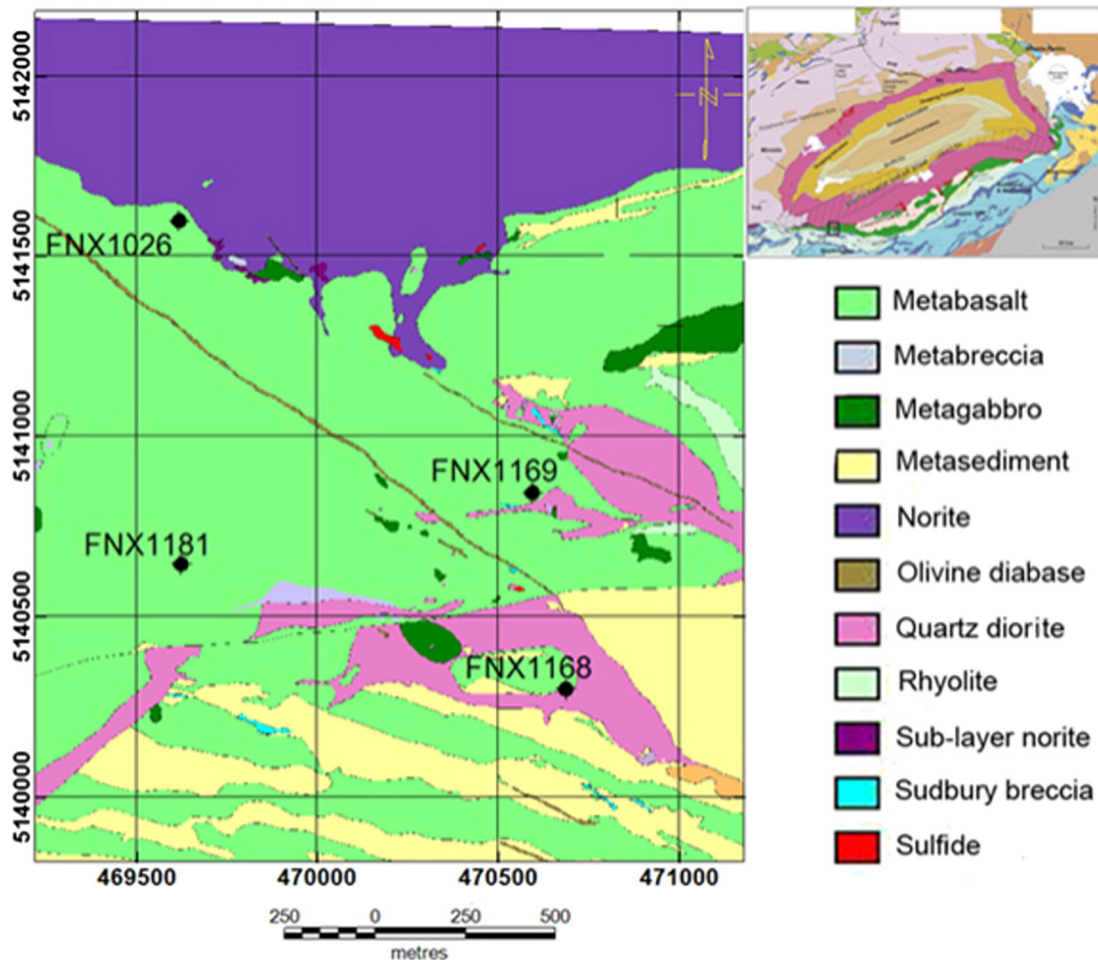


Fig. 2. The location of FNX1168 on the geological map of the Victoria property. FNX1182 is located to the north beyond the area covered by this map. The study area is marked by the small black rectangle in the top right figure.

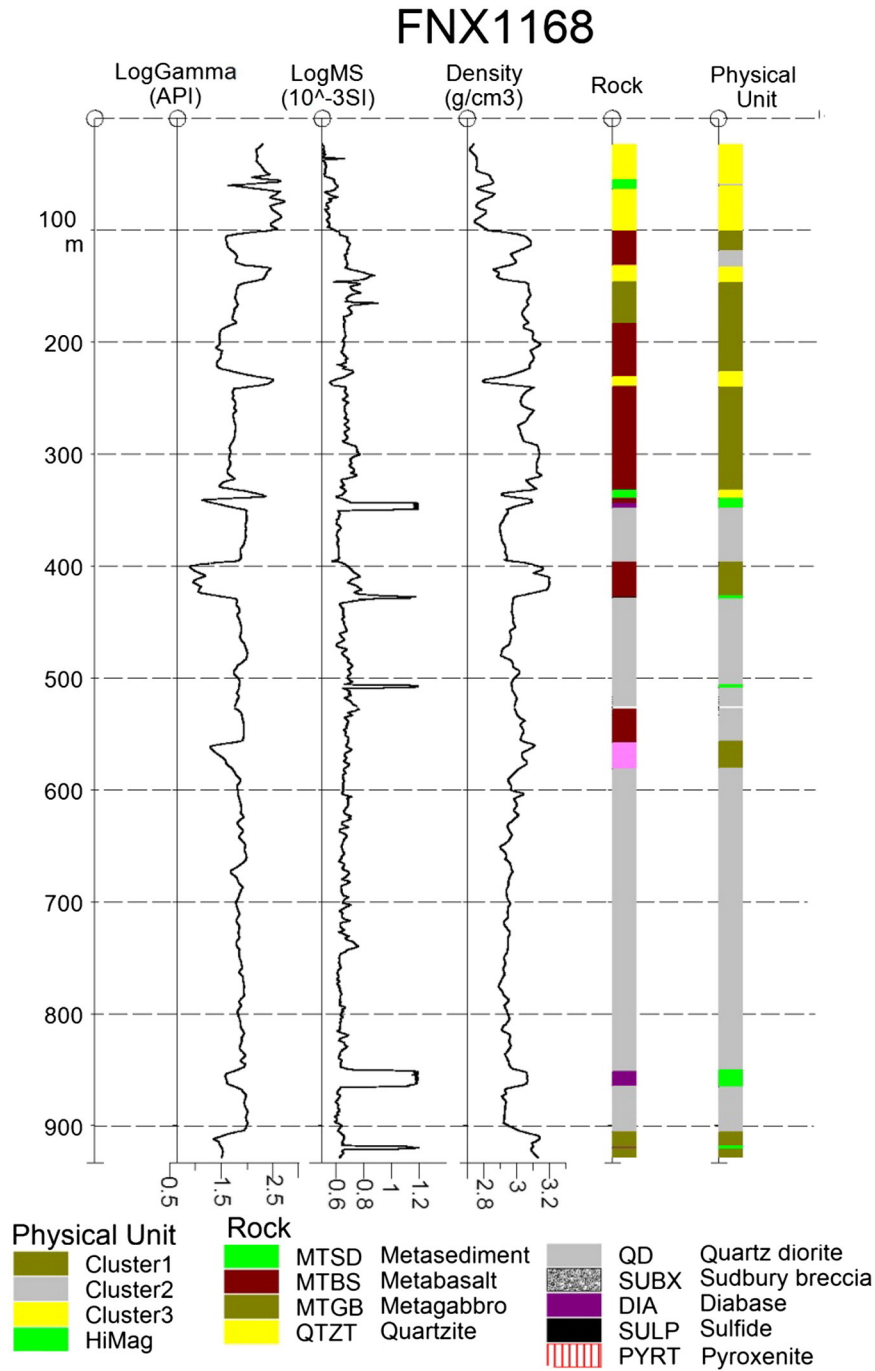


Fig. 3. Gamma-ray response, magnetic susceptibility and density measurement in FNX1168. These properties were used to train the network to predict the rock types logged by geologists (second from right panel) or the physical log units identified by fuzzy k-mean clustering (Mahmoodi and Smith, 2015) (right panel).

76th epoch and training was terminated at the 86th epoch where the maximum number of validation checks was reached. Overall, the network showed 83% correlation between the predicted rocks and the actual rocks during the training process. The confusion matrix in Table 1 shows the accuracy of the network in classification of individual rock types.

The homogenous rock types (rocks with spatially consistent physical properties), such as quartz diorite shows a high predictive accuracy. The accuracy for metabasalt, quartzite, quartz diorite, and diabase is remarkably high with 81, 97, 95, and 93% of cases predicted correctly. On the other hand, heterogeneity in rock types results in a large range of variability of physical properties and more overlap between rock types. Metasediment, metagabbro, and sulfide are completely misclassified,

as they are predicted as other rock types with similar physical properties. For example metasediment is usually predicted as quartzite; metagabbro is predicted as metabasalt; and sulfide is predicted as diabase.

Considering the prediction of similar rock types in Table 1, a question arises as to why metasediment is predicted as quartzite, and not vice versa. It turns out that the network shows preference for one rock type in the classification. The rock type with higher population contributes more data for training and controls the network parameters. Since quartzite is more dominant than metasediment, the network favors a choice for quartzite over metasediment; likewise, sulfide is predicted as diabase. Benaouda et al. (1999) incorporated the same number of samples from each class to avoid a bias caused by the larger populations

Table 1
Confusion matrix for the training data in hole FNX1168. The rock types logged by geologists (desired output) and predicted rock types by the neural network are represented in rows and columns, respectively. The percentage of contribution of actual rock types in each predicted rock types is summarized in the table. The total length of logged and predicted rock types are listed in last column and last row, respectively.

| | | Predicted rock types | | | | | | | Length (m) |
|-------------------|----------------|----------------------|-------------|-------------|---------------|-----------|---------|---------|------------|
| | | Quartz diorite | Meta-gabbro | Meta-basalt | Meta-sediment | Quartzite | Diabase | Sulfide | |
| Actual rock types | Quartz diorite | 95 | 0 | 4 | 0 | 0 | 1 | 0 | 455 |
| | Metagabbro | 11 | 1 | 88 | 0 | 0 | 1 | 0 | 59.8 |
| | Metabasalt | 18 | 0 | 81 | 0 | 1 | 0 | 0 | 235.6 |
| | Metasediment | 29 | 0 | 8 | 0 | 64 | 0 | 0 | 16 |
| | Quartzite | 3 | 0 | 0 | 0 | 97 | 0 | 0 | 93.2 |
| | Diabase | 4 | 0 | 3 | 0 | 0 | 93 | 0 | 20.4 |
| | Sulfide | 0 | 0 | 20 | 0 | 0 | 80 | 0 | 1 |
| | Length (m) | 492.2 | 1 | 262.6 | 0 | 102.6 | 22.6 | 0 | |

when training the neural network. But they concluded that this approach under-represents the larger classes which has an even greater detrimental impact on the results.

After the training process the parameters of the network are frozen and are then applied to data in FNX1182. The input data vector for each depth is presented to the network, and the 7-array output vector is produced. Each element in the output vector represents the predicted rock type probability, and the maximum probability determines the predicted rock type at a specific depth (Qi and Carr, 2006). The physical properties, predicted rock types, and actual rock types logged by the geologists in FNX1182 are represented in Fig. 4.

Comparison of the actual rock types and the predicted rock types shows that they have a 64% overall correlation. The predictive accuracy for individual rock types in FNX1182 is summarized in Table 2. Three-dimensional (3D) cross plots of physical properties in actual rock types (Fig. 5) and predicted rock types (Fig. 6) are presented. The box plots in Fig. 7 also depict the range of variation of physical properties (normalized between 0 and 1) in actual and predicted rock types of FNX1182.

As shown in Fig. 5 quartz diorite forms a dense, well separated class which facilitates classification of this rock type. The predicted quartz diorite has similar distribution in Fig. 6 as 98% of quartz diorite logged by geologists was predicted as quartz diorite in the neural network classification. Such a high correlation is illustrated by a similar range of physical properties of actual quartz diorite and predicted quartz diorite in Fig. 7.

Metagabbro and metabasalt have similar physical properties illustrated with significant overlap in Fig. 5. Table 2 shows that 44% and 43% of actual metagabbro and metabasalt are predicted correctly as metagabbro and metabasalt, respectively. Dissimilar distribution of these rock types in Figs. 5 and 6 illustrates their misclassification. However, they are mutually predicted as each other, i.e. 35% of both actual metagabbro and metabasalt are predicted as metabasalt and metagabbro, respectively. It implies that the network is not capable of distinguishing between rocks with similar physical properties.

High gamma-ray response and low density are the main characteristics of metasediment and quartzite in FNX1168, but Fig. 7 illustrates that they have a broader range of variation in FNX1182, which results in these rocks being predicted as metagabbro and quartz diorite. Due to similarity in physical properties of metasediment and quartzite 44% of metasediment is predicted as quartzite. Quartzite is relatively well classified with 55% receiving the correct classification.

Only 23% of diabase is correctly predicted by the neural network. High density and high magnetic susceptibility are the characteristics of diabase in FNX1168. However in FNX1182, as shown in Fig. 7, the main portion of this rock has a lower density and is surrounded in Fig. 4 by quartz diorite and metagabbro. This means that diabase in FNX1182 have different properties from the diabase used in the training process, so are predicted to be quartz diorite (52%) and metagabbro

(25%). Inconsistent physical properties of diabase result in inaccurate performance of the network for diabase prediction. Measurements of other rock types with high magnetic susceptibility are predicted as diabase.

Due to insufficient samples in the training process and similar physical properties of sulfide and diabase, sulfide is mainly (75%) predicted as diabase. Distribution of sulfide in Fig. 5 corresponds to predicted diabase in Fig. 6. Sudbury breccia and pyroxenite are three rock types in FNX1182 which are absent in FNX1168. So, the trained network is not capable of predicting these rocks. Their physical properties are such that they are predicted as other rock types. Pyroxenite is mainly predicted as quartz diorite and to some extent as metagabbro and metabasalt. Sudbury breccia is the most heterogeneous rock and does not show consistent physical properties (Fig. 5) and its contribution to different predict rock types can be seen in Table 2.

4.2. Predicting physical log units

The second approach is to represent the physical properties measurements of FNX1182 with physical log units. A 3-10-4 network was selected for physical log unit prediction in FNX1182. Physical properties measurements and identified physical log units from FNX1168 (Fig. 3) were used to train the network. Cluster 1 has low gamma ray response and high density; cluster 2 is characterized by medium gamma ray response and medium density; cluster 3 shows low density and high gamma-ray response; and a HiMag unit is distinguished by high magnetic susceptibility. A careful comparison of the physical log units with the geological rock type from FNX1168 (Mahmoodi and Smith, 2015) concluded that cluster 1 mainly represents metabasalt and metagabbro, cluster 2 constitutes quartz diorite, cluster 3 mainly represents metasediment and quartzite, and HiMag represents diabase and sulfide.

In the training process, the best validation performance occurred at the 61st epoch where the training stopped as the minimum gradient was reached. The more rapid convergence than training the network for rock-type prediction suggests the reduced complexity of the problem.

The confusion matrix for the training data in Table 3 shows that the physical log units have a total of 95% of the samples being correctly classified. Thus, the ambiguity associated with the rock-type prediction that resulted in misclassifications is not seen with physical log units.

The neural network was then applied to the physical properties measurements collected in FNX1182 and each input datum was classified as either cluster 1, 2, 3, or the HiMag unit (Fig. 4, the right column). Fig. 8 shows distribution of physical units in the physical properties environment.

In addition to being used in geophysical studies, the predicted physical units can be used in conjunction with available geological information. The reliability of this approach mainly relies on our understanding of the link between physical units and rock types. We assume that the

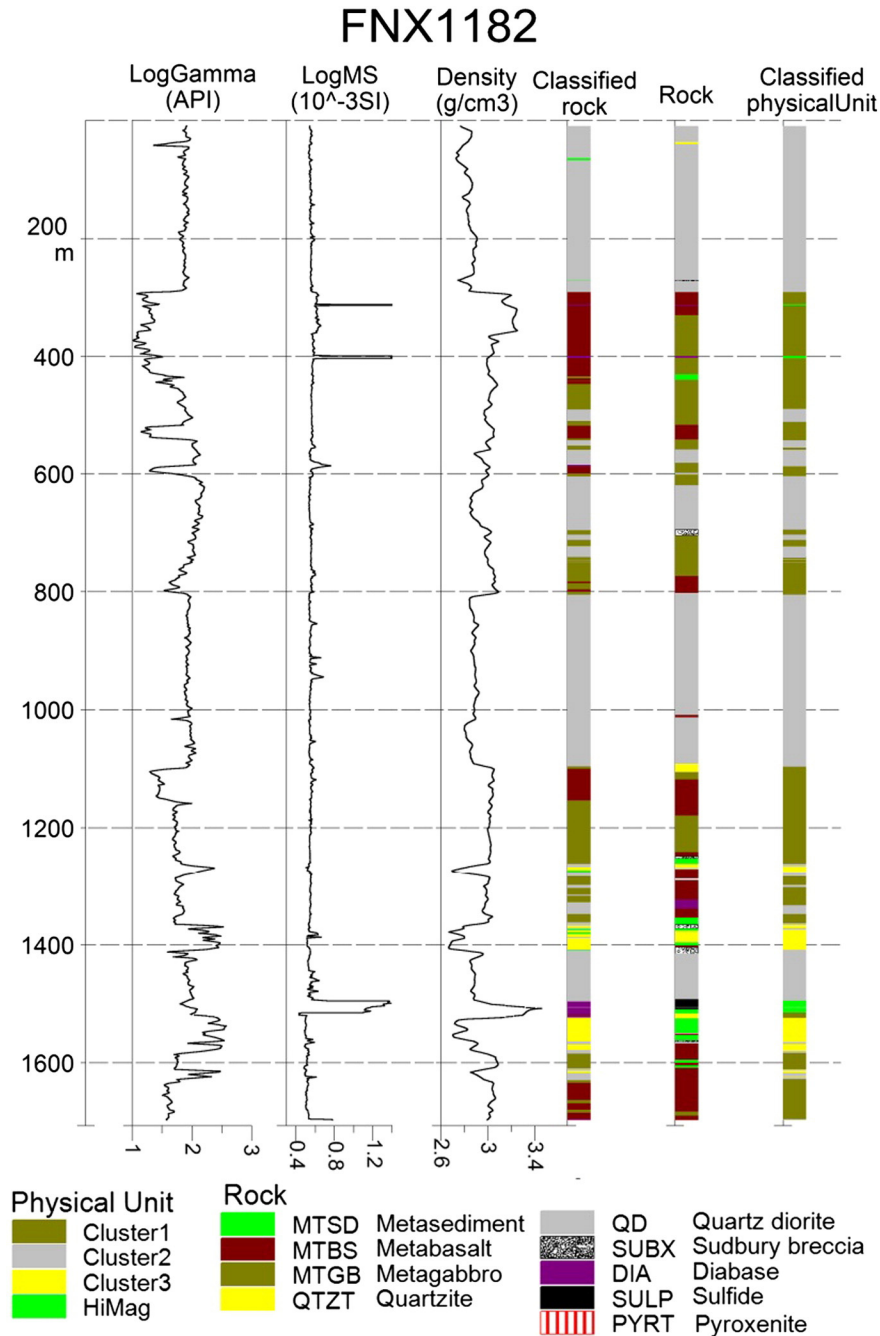


Fig. 4. Gamma-ray response, magnetic susceptibility and density measurement in FNX1182, which were presented to the trained network. Predicted rock types (third from right panel) and physical log units (right panel) are plotted. The geologist’s classified rock types (second from right panel) are shown for comparison purpose.

same relationships between the physical units and rock types apply to FNX1182. To verify this assumption the predicted physical units were compared with the actual rock types in FNX1182 and the contribution of each rock types in the four physical units is summarized in Table 4. The results mostly agreed with the expected correlation of physical units with rock types. This implies that physical unit prediction can be used as a tool to identifying classes of rock types with acceptable certainty.

Specifically, ninety eight percent of quartz diorite in FNX1182 is represented by cluster 2. Quartzite and typical metasediment with high gamma-ray response are the dominant rock types in cluster 3 with 70% and 45% contributions, respectively. Cluster 1 represents 77% of metagabbro and 80% metabasalt. Unlike in hole FNX1168, a high portion

of diabase is classified into cluster 1. Sulfide was mainly represented in the HiMag cluster.

5. Discussion

Several factors should be considered while interpreting predicted rock types directly from physical properties or inferred from physical unit prediction.

- While training the network, the number of data belonging to each class involved in the training process influences the network performance. Because the rock types with a large population contribute more data in training, the network shows a preference for the

Table 2
The rock types logged by geologists (left column) were considered to evaluate the network accuracy in rock type prediction in hole FNX1182. The rock types predicted by the neural network are represented in columns, and the percentage of contribution of actual rock types in each predicted rock types is summarized in the table. Total length of logged and predicted rock types are listed in last column and last row, respectively.

| | Predicted rock types | | | | | | | | Length (m) |
|-------------------|----------------------|----------------|-------------|-------------|---------------|-----------|---------|---------|------------|
| | | Quartz diorite | Meta-gabbro | Meta-basalt | Meta-sediment | Quartzite | Diabase | Sulfide | |
| Actual rock types | Quartz diorite | 98 | 1 | 0 | 0 | 1 | 0 | 0 | 754 |
| | Metagabbro | 20 | 44 | 35 | 0 | 0 | 1 | 0 | 378.2 |
| | Metabasalt | 15 | 35 | 43 | 1 | 6 | 1 | 0 | 349.2 |
| | Metasediment | 5 | 35 | 7 | 2 | 44 | 7 | 0 | 89 |
| | Quartzite | 23 | 1 | 2 | 8 | 55 | 13 | 0 | 33.6 |
| | Diabase | 52 | 25 | 0 | 0 | 0 | 23 | 0 | 20 |
| | Sudbury breccia | 40 | 31 | 0 | 3 | 27 | 0 | 0 | 39.2 |
| | Sulfide | 25 | 0 | 0 | 0 | 0 | 75 | 0 | 15.8 |
| | Pyroxenite | 47 | 21 | 31 | 0 | 0 | 0 | 0 | 17.8 |
| | Length(m) | 913.6 | 350.8 | 295.4 | 13 | 92 | 32 | 0 | |

dominant rock type rather than less populous rock types when they have similar physical properties. Thus, the significant prediction of metasediment as quartzite, or sulfide as diabase can be explained, as in each case, the latter rock-type is more populous.

- Another factor is the heterogeneity of rock types which results in inconsistent physical property behavior. If the physical properties of a specific rock type are different in the training data and the prediction data, the rock type cannot be predicted correctly. The high density and high magnetic susceptibility are two distinguishing characteristics of diabase, but a remarkable portion of diabase in FNX1182 has lower density and magnetic susceptibility. This results in misclassification of diabase as quartz diorite and metagabbro. Another example of this is the misclassification of metasediment as metagabbro in FNX1182.
- Similarity in physical properties results in ambiguity. The overlap of physical properties of two or more rocks results in misclassification. Metagabbro and metabasalt are misclassified as each other in rock type prediction, and they are represented by one physical unit.
- The network is able to predict only the rock type or physical log units from which it is trained. Wise data selection for training the network

is therefore critical for accurate classification. Sudbury breccia and pyroxenite were not considered as an output in the rock type prediction because they were absent in the training data.

To find a geological explanation for the similarities and differences in the physical characteristics of rocks core samples were studied. Plagioclase, amphibole, and pyroxene are the dominant minerals of both metagabbro and metabasalt, though metabasalt contains slightly higher amount of amphibole and a smaller amount of biotite. The grain size of metabasalt is finer than metagabbro. Thus, they are of broadly similar composition and mineralogy, explaining the similar physical properties of these two rocks, and the differences in grain size appears to not control the physical properties as much as the mineralogy. A detailed examination of the metabasalt and metagabbro showed patches of inconsistent grain size and the percentage of clinopyroxene observed in core samples, possibly explaining some of the heterogeneity in the physical properties measurements.

Compared to metagabbro and metabasalt, quartz diorite contains less amphibole and pyroxene, and higher amounts of plagioclase and

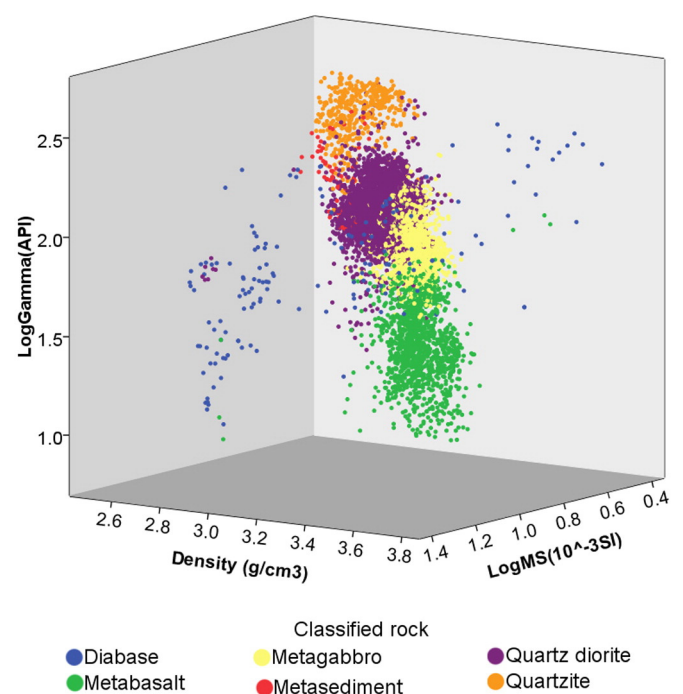
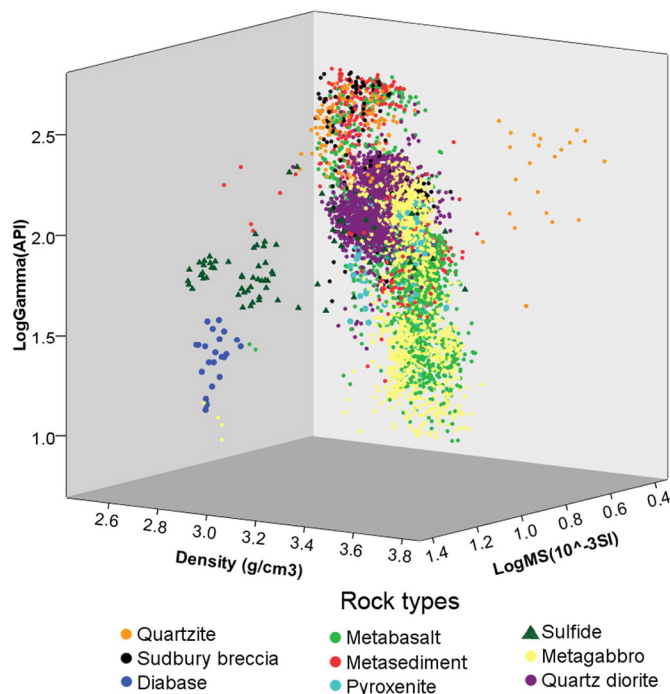


Fig. 5. 3D cross plots of density, gamma-ray response, and magnetic susceptibility measurements for the actual rock type in FNX1182.

Fig. 6. 3D cross plots of density, gamma-ray response, and magnetic susceptibility measurements for the predicted rock types in FNX1182.

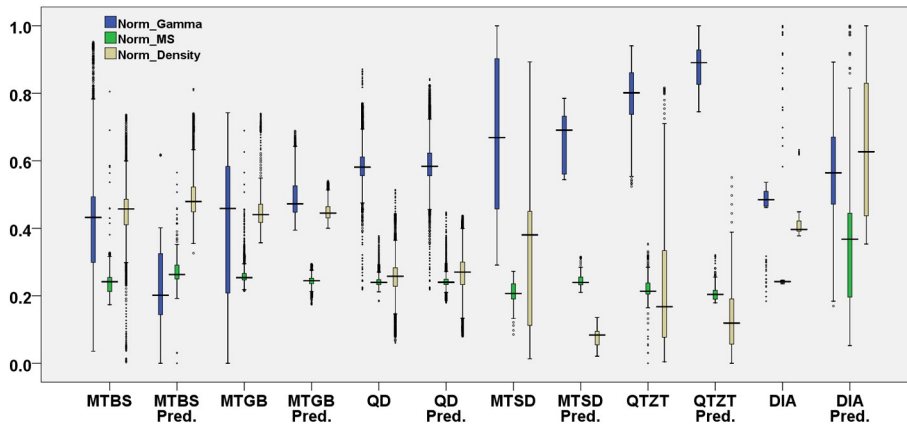


Fig. 7. Box-plots of normalized gamma ray response, magnetic susceptibility and density measurements of rock types logged by geologists and predicted by the neural network. Labels used in the plot: MTBS: metabasalt; MTGB: metagabbro; QD: quartz diorite; MTSD: metasediment; QTZT: quartzite; DIA: diabase.

quartz. It has finer grain size, is lighter in color, and has a lower density. Occurrences of sulfide mineralization in quartz diorite will increase its density, although for low concentrations of mineralization the increase is not significant enough to make a significant change in the density log.

Metasediment has a similar mineralogical composition to quartz diorite, but also contains minor garnet and iron oxide. The high gamma-ray response of the metasediment is interpreted to be due to the relatively high concentration of radioactive minerals in the protolith (sedimentary rocks that were metamorphosed).

Diabase has a fine grain size and is composed of pyroxene, amphibole, and up to 10% magnetite. Such high concentration of dense mafic minerals and magnetite increases the density and magnetic susceptibility of diabase. The portion of diabase with lower magnetic susceptibility contains less magnetite. Diabase can be mineralogically very similar to gabbro, which explains why the non-magnetic diabase is predominantly placed in cluster 1 containing metagabbro and metabasalt. Metamorphism can result in changes in the amount and grain size of magnetite and variable metamorphism could play a role in the classification of diabase, metagabbro and metabasalt. High concentration of pyrrhotite also increases the magnetic susceptibility which corresponds to the sulfide zone on the log with high magnetic susceptibility.

Pyroxenite is a rock primarily composed of the mafic mineral pyroxene which explains why it is easily misclassified as a metagabbro or a basalt (which also contain pyroxene) when there are few radioactive minerals present, or quartz diorite when there are more radioactive minerals present. The Sudbury breccia forms via cataclasis of pre-existing rocks and can form in any of the other rock types present in the area. The formation of the breccia produces a finer-grained matrix and clasts that simply reflect a mixture of the pre-existing rock types, explaining the heterogeneity and the difficulty in classifying this rock type.

Table 3
Correlation between physical log units defined by fuzzy k-means clustering (rows) and predicted by the neural network (columns) using the training data set from FNX1168. The values indicate the percentage of contribution of the defined physical units in each of the predicted unit. The total length of drill-hole classified to each of the units is shown in the table.

| | Predicted physical unit | | | | |
|---|-------------------------|-----------|-----------|-------|-----------|
| | Cluster 1 | Cluster 2 | Cluster 3 | HiMag | Length(m) |
| Physical units identified by clustering | Cluster1 | Cluster2 | Cluster3 | HiMag | Length(m) |
| | 95 | 3 | 0 | 2 | 268.4 |
| | 1 | 98 | 1 | 0 | 495.2 |
| | 1 | 2 | 97 | 0 | 109.6 |
| | 1 | 4 | 0 | 95 | 31.2 |
| | 263.4 | 494.6 | 112.2 | 34.2 | |

The confusion associated with rock-type prediction is due to the overlap between the physical properties of the rock types, and this reduces the reliability of the results. If the rocks with similar physical properties are represented as a physical log unit, the problem is simplified. The significant decrease in the number of misclassified data in the process of training the network to identify physical log units illustrates greater accuracy and reliability (Table 3). In this case, although there are fewer types classified, interpretation can be more reliable since there is less ambiguity associated with the results.

6. Conclusion

Depending on the objective, down-hole physical properties measurements can be analyzed using the neural network to predict geological rock type or determine physical log units in the hole. The heterogeneity of physical property of rocks and the overlap of the physical properties of two or more rock types reduce the prediction accuracy. The population of rock types also controls the training process as the network shows preference for dominant rock types in the output and

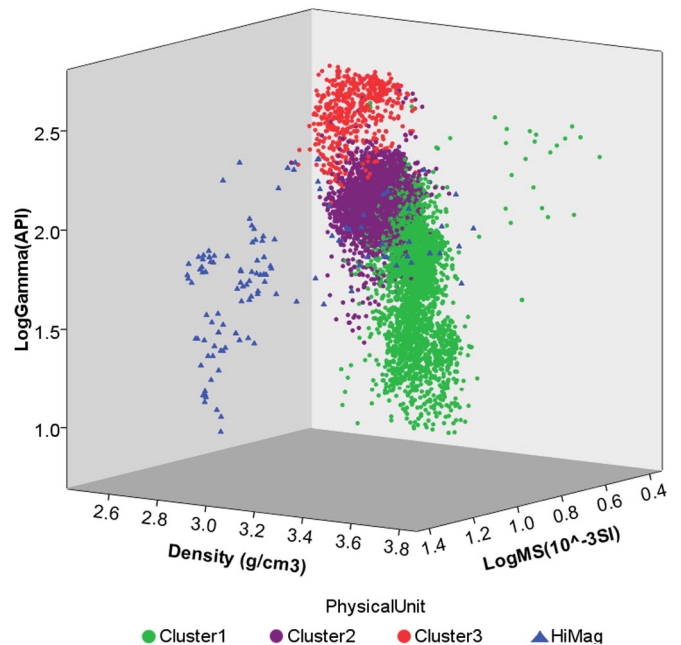


Fig. 8. 3D cross plots of density, gamma-ray response, and magnetic susceptibility measurements for the predicted physical units in FNX1182.

Table 4

The percentage contribution of rock types (logged by geologists) as classified into physical log units in FNX1182.

| | Predicted physical units | Cluster | | | HiMag | Length (m) |
|--|--------------------------|-------------------|----------------|-----|-------|------------|
| | | 1 | 2 | 3 | | |
| | | Actual rock types | Quartz diorite | 1 | | |
| | Metagabbro | 77 | 22 | 0 | 0 | 378.2 |
| | Metabasalt | 80 | 12 | 8 | 0 | 349.2 |
| | Metasediment | 45 | 4 | 45 | 5 | 89 |
| | Quartzite | 17 | 13 | 70 | 0 | 33.6 |
| | Pyroxenite | 49 | 51 | 0 | 0 | 17.8 |
| | Diabase | 49 | 28 | 0 | 23 | 20 |
| | Sulfide | 0 | 16 | 0 | 84 | 15.8 |
| | Sudbury breccia | 34 | 32 | 34 | 0 | 39.2 |
| | Length (m) | 661 | 902.6 | 109 | 24.2 | |

minor rock types are predicted as the dominant rock types that have most similar physical properties.

In this work, the network was trained from data from FNX1168 to obtain the appropriate network to predict rock types and physical units in FNX1182. Predicting the physical units was simpler compared with rock type prediction, requiring only 10 hidden neurons compared with 15. When predicting the rock type, an accuracy of 83% was achieved in the training process, which is reasonable considering the complexity of this problem. However, the trained network only had 64% of accuracy in predicting rock types in FNX1182. There was an accuracy of 95% in training the network on physical log units (defined by a fuzzy k-means statistical classification), which implies an enhanced reliability and less ambiguity of the results.

In geological or geophysical studies, physical properties can be used to predict either rock type or physical units. Using a neural network to predict rock type instead of physical units gives more detailed information, however the tradeoff is less accuracy and greater ambiguity. On the other hand, when predicting the physical log unit, there is greater accuracy, but the ambiguity is still not completely resolved, as many different rocks can be classified as a single physical log unit depending on the exact factors controlling the geophysical properties. However, the physical log units do define identifiable and unique units with geological significance from a physical properties perspective, and these can be useful for geophysical studies in forward and inverse modeling exercises.

Acknowledgments

We are grateful to NSERC (405646 - 09), Vale, Sudbury Integrated Nickel Operations, A Glencore Company, KGHM International, Wallbridge Mining and the Centre for Excellence in Mining Innovation for funding this research. Specifically we would like to acknowledge KGHM International for providing the data for this study; Bill Spicer of KGHM International and Vince Gerrie of DGI for their support.

References

- Baldwin, J., Bateman, A., Wheatley, C., 1990. Application of neural network to the problem of mineral identification from well logs. *Log. Anal.* 31, 279–293.
- Beale, M., Hagan, M., Demuth, H., 2001. *Neural Network Toolbox User's Guide R2014a*. The Math Works Inc., Natick.
- Benaouda, D., Wadge, G., Whitmarsh, R.B., Rothwell, R., MacLeod, C., 1999. Inferring the lithology of borehole rocks by applying neural network classifiers to downhole logs: an example from the Ocean Drilling Program. *Geophys. J. Int.* 136, 477–491.
- Bishop, C., 1995. *Neural Networks for Pattern Recognition*. Oxford University, New York.
- Duda, R.H., 2001. *Pattern Classification*. Wiley, New York.
- Farmer, R., Adams, S.J., 1998. *Facies Recognition Using Neural Networks*. New Zealand Petroleum Conference, Queenstown.
- Garcia, M.H., Rabaute, A., Yven, B., Guillemot, D., 2011. Multivariate and spatial statistical analysis of Callovo-Oxfordian physical properties from lab and borehole logs data: towards a characterization of lateral and vertical spatial trends in the Meuse/Haute-Marne Transposition Zone. *Phys. Chem. Earth* 36, 1469–1485.
- Graneck, J., 2011. *Computing Geologically Consistent Models from Geophysical Data*. University of British Columbia, BC, Canada.
- Killeen, P., 1997. Borehole geophysics: exploring the third dimension. In: Gubins, A. (Ed.), *Exploration 97: Fourth Decennial International Conference on Mineral Exploration*, pp. 31–42.
- Lawrence, S., Giles, C.L., Tsoj, A.C., 1996. What Size Neural Network Gives Optimal Generalization? Convergence Properties of backpropagation. Institute for Advanced Computer Studies. College Park: University of Maryland.
- Mahmoodi, O., Smith, R., 2015. Clustering of downhole physical properties measurements at the Victoria property, Sudbury for the purpose of extracting lithological information. *Journal of Applied Geophysics* 118, 145–154.
- Maiti, S., Tiwari, R.K., Kumpel, H.J., 2007. Neural network modelling and classification of lithofacies using well log data: a case study from KTB borehole site. *Geophys. J. Int.* 169, 733–746.
- McDowell, G., Fenlon, K., King, A., 2004. Conductivity-based nickel grade estimation for grade control at Inco's Sudbury mines. SEG Annual Meeting, Denver, Colorado.
- McDowell, G.M., King, A., Lewis, R.E., Clayton, E.A., Grau, J.A., 1988. In-situ nickel assay by prompt gamma neutron activation wireline logging. SEG Annual Meeting, New Orleans, Louisiana.
- Mwenifumbo, C., Mwenifumbo, A., 2012. Borehole geophysical logging in the Flin Flon Mining Camp. Geological survey of Canada. *Geol. Surv. Can.* 75.
- Ojha, M., Maiti, S., 2013. Sediment classification using neural networks: an example from the site-U1344A of IODP Expedition 323 in the Bering Sea. *Deep-Sea Res. II*.
- Perron, G.F., Phillips, N., Williston, C., Gerrie, V., Everest, J., 2011. 3D litho-prediction model from in-situ physical rock property logging and constrained potential fields data inversion. 31st Gocad Meeting, Nancy.
- Qi, L., Carr, T.R., 2006. Neural network prediction of carbonate lithofacies from well logs, Big Bow and Sand Arroyo Creek fields, Southwest Kansas. *Comput. Geosci.* 32, 947–964.
- Rabaute, A., Yven, B., Chelini, W., Zamora, M., 2003. Subsurface geophysics of the Phlegrean fields: new insights from downhole measurements. *Geophys. Res.*
- Reed, L., Taneer, M., Elliott, B., Killeen, P., 1997. A comparison of physical property borehole logs with geology, mineralogy and chemistry in a borehole at Les Mines Selbaie, northwestern Québec, Canada. In: Gubins, A. (Ed.), *Exploration 97: Fourth Decennial International Conference on Mineral Exploration*, pp. 1043–1048.
- Theodoridis, S., Koutroumbas, K., 2003. *Pattern Recognition*. 2nd ed. Academic Press, New York.
- Vella, L., Emerson, D., 2009. Carrapateena: physical properties of a new iron-oxide copper-gold deposit. *Journal Article ASEG Extended Abstracts*, pp. 1–13.
- Williams, N., Dipple, G., 2007. Mapping subsurface alteration using gravity and magnetic inversion models. In: Milkereit, B. (Ed.), *Exploration 07: Fifth Decennial International Conference on Mineral Exploration*, pp. 461–472.
- Wong, P., Jian, F., Taggart, L., 1995. A critical comparison of neural networks and discriminant analysis in lithofacies, porosity and permeability predictions. *J. Pet. Geol.* 18 (2), 191–206.